

THE USE OF VATERITE AS A TRAP FOR METALLIC IONS IN WATER STUDY OF COPPER/VATERITE AND MANGANESE/VATERITE SYSTEMS

Samer Aouad, Elias Saab¹, Najat Nassrallah-Aboukaïs¹, Edmond Abi-Aad¹ and Antoine Aboukaïs¹

Department of Chemistry, Faculty of Sciences, University of Balamand, P.O.Box 100,
Tripoli, Lebanon

¹ Laboratoire de Catalyse et Environnement, E.A. 2598, MREI, Université du Littoral – Côte
d'Opale, 145, avenue M. Schumann, 59140 Dunkerque, France
samer.aouad@balamand.edu.lb

(Received 24 June 2008 - Accepted 24 January 2009)

ABSTRACT

The crystalline transformation of vaterite into cubic calcite can be carried out under the influence of various aqueous solutions present in nature (tap water, various mineral water). It can also be performed due to heating under air or inert atmosphere. During its transformation, the vaterite can trap ions present in the aqueous medium. UV-Vis/NIR and EPR analyses carried out on samples recovered after reaction with different solutions of Cu^{2+} and Mn^{2+} show the presence of these ions in the structure of calcite after transformation. That demonstrates the capacity of vaterite to imprison metal ions during its transformation into cubic calcite. Mn^{2+} EPR signals detected after reaction of vaterite with demineralized water confirms trapping efficiency of vaterite in the presence of low ions contents.

Keywords: cubic calcite, Cu^{2+} , DSC, EPR, Mn^{2+} , trap, vaterite, UV-Vis/NIR

INTRODUCTION

The adsorption of ionic species on carbonates and their evolution represent for the scientists an important aspect of the grounds and aquatic environments geochemistry. The matter exchange on the liquid-carbonates interface are described by the traditional rules of the heterogeneous kinetics according to a complex reaction pathway bringing into play precipitation, germination (nucleation) then crystal growth. In addition, the exchange reactions on the interface "natural water-carbonates" are more or less disturbed by foreign ions which, according to the type of carbonate brought into play in the medium, will involve changes in the orientation of crystallization towards different system (Reeder, 1983; Morse & Mackenzie, 1990; Stumm, 1992). The comprehension of these phenomena is very important with an aim of using carbonates as traps for metal ions in the aqueous mediums and to decontaminate these latter thereafter. The natural calcium carbonate exists mainly in two different but thermodynamically very close crystalline forms: calcite (rhombohedral) and

aragonite (orthorhombic). Another polymorph of CaCO_3 also exists with less important contents, it is the vaterite. This latter is metastable because it changes irreversibly in contact with water giving calcite or aragonite (Bischoff, 1968).

In this work, the capacity of vaterite to trap metal ions during its transformation into calcite in aqueous mediums is studied. This transformation was made in the presence of Cu^{2+} and Mn^{2+} ions in the aqueous mediums.

MATERIALS AND METHODS

Cu^{2+} / vaterite and Mn^{2+} / vaterite samples with various Cu(II) or Mn(II) contents were prepared by addition of 10 mL of various $\text{Cu}(\text{NO}_3)_2 \cdot 3\text{H}_2\text{O}$ (Acros organics; purity 99%) or $\text{Mn}(\text{NO}_3)_2 \cdot 4\text{H}_2\text{O}$ (Acros organics; purity 97.5 %) solutions (10^{-5} ; 10^{-4} ; 10^{-3} ; 10^{-2} and 10^{-1}M) on 300 mg of vaterite (Acros organics, purity 99%). The “metal/vaterite” mixtures are agitated to obtain homogeneous carbonates phases at 293 K.

Scanning electron microscopy (SEM) images were performed on a JEOL JSMT 330A microscope. Samples are crushed out into fine powder which is suspended in water thereafter.

Electron paramagnetic resonance (EPR) measurements were performed with an EMX Bruker spectrometer with a cavity operating at a frequency of $\sim 9.5\text{GHz}$ (X band). The magnetic field was modulated at 100 kHz and the power supply was sufficiently small to avoid saturation effect. The measurements were performed at room temperature and at 77 K. The g values were determined from precise frequency and magnetic field values. EPR intensity was given by the normalized double integration of the EPR signal.

Thermal analysis measurements were performed using a Netsch STA 409 apparatus equipped with a microbalance (TG), differential scanning calorimetry (DSC) and a gas flow system. Solids were treated under a flow of dry air (75 mL/mn). Temperature was raised at a rate of $5^\circ\text{C}/\text{mn}$ from room temperature to the desired temperatures.

UV-VIS/NIR diffuse reflectance spectra were recorded using a Varian Cary 5000 spectrophotometer.

RESULTS AND DISCUSSIONS

Figure 1 shows SEM images of solid samples recovered after various reaction times in Milli-Q Plus water and dried during one night at 373 K. Vaterite crystals are initially in the form of spheres or pseudo-spheres with diameters ranging between 0.5 and 5.0 μm . During the crystalline transformation, these spheres change gradually because of calcite cubic formation. These new crystals present dimensions varying from 1.5 to 4.5 μm . During this process, vaterite grains agglomerate giving larger particles ranging between 2.5 and 5.5 μm before they transform completely into cubic calcite. The completion of this transformation requires a reaction time of at least 24 h. In a more simple way, the reaction mechanism consists of 3 stages: (i) a progressive dissolution of small vaterite crystals on the grains surface; (ii) generation of cubic calcite micro-germs (thermodynamically more stable than vaterite) in the liquid phase; and finally (iii) a precipitation of cubic calcite giving crystals of rhombohedral forms.

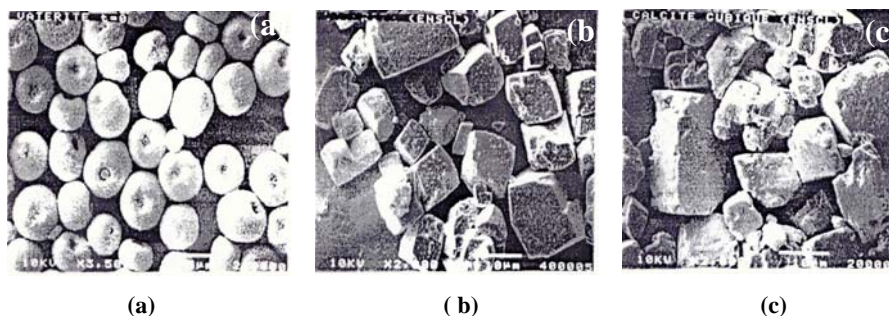


Figure 1. SEM images showing the solids morphological evolution during the crystalline transformation of vaterite into suspension in Milli-Q Plus water.

Time of reaction: a) 0 h; b) 24 h; c) pure calcium carbonates "cubic calcite".

It is also known that vaterite can transform into cubic calcite under heating in the presence and in the absence of oxygen (Nasrallah-Aboukais *et al.*, 2003). Figure 2a illustrates the TG and DSC curves of the pure vaterite sample after heating the solid under a flow of dried air. The DSC curve reveals three exothermic peaks at 261, 481 and 488°C and an endothermic peak at 775°C. The exothermic peaks were obtained without any mass loss. On the contrary, the endothermic peak was accompanied with a large mass loss (44%). This loss corresponds exactly to the decomposition of solid CaCO_3 into CaO and CO_2 .

When vaterite is in contact with demineralised water (Figure 2b), only the endothermic peak at 767°C was observed. It is important to state that no modification was noticed for the mass loss corresponding to this latter.

In the literature (Perić *et al.*, 1996; Baitalow *et al.*, 1998; Wolf *et al.*, 2000), the two exothermic peaks obtained at 481 et 488°C are unambiguously attributed to the transformation of vaterite into calcite. In fact, the pure vaterite used in this study, already contained a small amount of calcite on its surface due to the direct contact with air humidity. For this reason, two types of vaterite are created in these solids: the first one is directly in contact with the calcite phase and the other one can be considered as pure because it is far from the calcite phase (Nasrallah-Aboukais *et al.*, 2003). This is confirmed by the DSC curve of vaterite kept in contact with demineralised water for 7 days, as no such exothermic peaks appeared, indicating the absence of vaterite phase in the recuperated solid. As for the 216°C exothermic peak, an earlier study (Nasrallah-Aboukais *et al.*, 2003) confirmed that it is closely correlated to the interaction between oxygen and the vaterite surface which can explain its absence in Figure 2b where the transformation of vaterite into cubic calcite is already achieved.

Figure 3 shows the EPR spectra evolution of Mn^{2+} /vaterite mixtures with the Mn^{2+} ion concentration after reaction times of 2 hours and 7 days. It is observed that for low Mn^{2+} concentrations (10^{-5} and 10^{-4}M), the general shape of the observed spectra corresponds well to the descriptions made in the literature for Mn^{2+} ion, especially when this latter is incorporated in a calcium carbonate matrix. After 2 hours of contact between vaterite and low Mn^{2+} concentration solutions, EPR spectra show a hyperfine structure presenting six fine lines ($I=5/2$) with a hyperfine coupling constant A_{iso} of 95G and a g_{iso} of 1.9984 (Table 1).

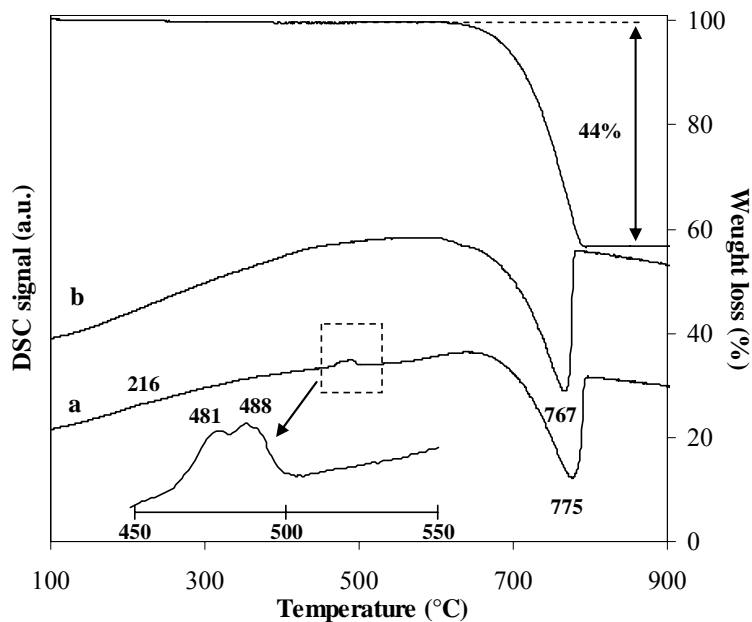


Figure 2. TG and DSC curves of a) pure vaterite ; b) vaterite in contact with demineralised water during 7 days.

For 10^{-3} M manganese (II) solution, and after 2 hours, a broad symmetrical signal ($\Delta H \sim 328G$) centred at $g = 2.003$ is detected. This latter is attributed with no ambiguity to the paramagnetic resonance of Mn^{2+} ions in strong dipolar interactions $Mn^{2+}-Mn^{2+}$. For high manganese (II) concentrations (10^{-2} and $10^{-1}M$), EPR spectra present broad symmetrical signals with $g = 2.005$ (Wartel *et al.*, 1990; Boughriet *et al.*, 1992; Rivaro *et al.*, 1994).

TABLE 1

Paramagnetic Parameters Obtained from EPR Spectra of the Different Mn^{2+} Samples after 2 Hours and 7 Days

| | [M] | 2 hours | | | 7 days | | |
|------------------|-----------|---------|---------------|----------------|--------|---------------|----------------|
| | | g | A_{iso} (G) | ΔH (G) | g | A_{iso} (G) | ΔH (G) |
| Mn ²⁺ | 10^{-5} | 1.998 | 95 | - | 2.000 | 95 | - |
| | 10^{-4} | 1.998 | 95 | - | 1.998 | 95 | - |
| | 10^{-3} | 2.003 | - | 328 | 1.998 | 95 | - |
| | 10^{-2} | 2.005 | - | 328 | 1.998 | 95 | - |
| | 10^{-1} | 2.005 | - | 315 | 2.003 | - | 228 |

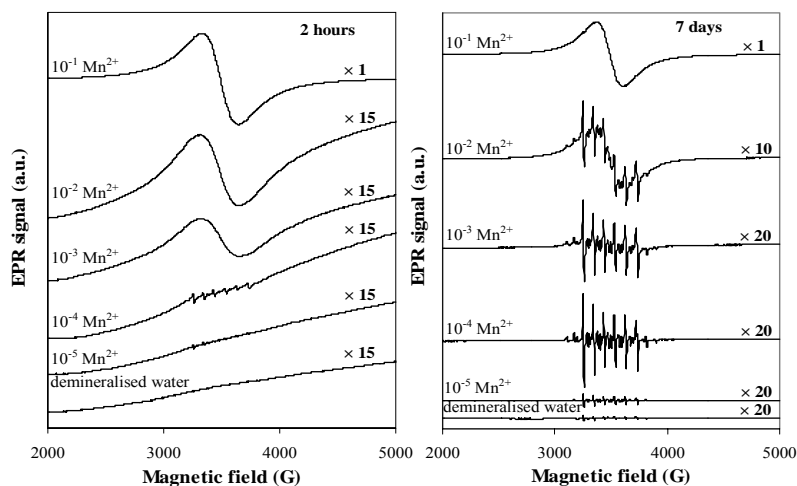


Figure 3. EPR spectra of the different Mn^{2+} /vaterite mixtures after 2 hours and 7 days of reaction.

After 7 days of reaction, the EPR spectra are very different from those obtained after 2 hours. For low Mn^{2+} concentrations, (10^{-5} and 10^{-4}M), the spectra always show hyperfine structure corresponding to manganese (II), but the signals are more intense compared to those obtained after 2 hours of reaction. After 7 days of reaction, and for the 10^{-3}M manganese (II) concentration, the broad signal observed after 2 hours disappears giving a new more intense signal with a hyperfine structure. This observation indicates clearly that in this latter case, all Mn^{2+} ions are isolated in the CaCO_3 matrix and thus are well dispersed in cubic calcite structure which is formed after transformation of vaterite. For the 10^{-2}M manganese (II) concentration, the broad signal is still present after 7 days but at the same time, a hyperfine structure appears and overlays the broad signal. This is due to the presence of isolated Mn^{2+} ions in cubic calcite but also to Mn^{2+} ions on the surface of cubic calcite. For greater manganese concentrations 10^{-1}M , only a broad signal is present after 7 days showing that the concentration of surface manganese ions is very high comparing to isolated manganese ions.

Figure 4 shows EPR spectra evolution of Cu^{2+} /vaterite mixtures with the Cu^{2+} ion concentration after reaction times of 2 hours and 7 days. For low cupric ions concentrations (10^{-5} and 10^{-4}M), the signal detected after 2 hours is characterized by a traditional axial symmetry with $g_{\parallel} > g_{\perp}$. This last corresponds to Cu^{2+} ions located in distorted octahedral symmetry sites (Aboukais *et al.*, 1992). According to the A value (Table 2), one can conclude that in this system each cupric ion is surrounded by five ligands (and not by six ligands) what leaves sufficient space to an oxygen gap.

After 7 days of reaction and for the same concentrations, the signal initially detected disappears and a new centred signal, with $g = 2.245$ and a line width of 40G for 10^{-5}M and 80G for 10^{-4}M , is observed. This isotropic broad signal is generally obtained when the dipolar interactions between the paramagnetic species are rather strong. Indeed, the reduction in specific surface during vaterite transformation into cubic calcite involves the

trapping of an important quantity of cupric ions, bringing paramagnetic species closer and thus the increase in the dipolar interactions between Cu^{2+} . For a 10^{-3}M cupric ions concentration, EPR spectrum of the recovered solid is similar to those detected previously for a vaterite/ Cu^{2+} mixtures (10^{-5} and 10^{-4} M) filtered after two hours. EPR parameters of this signal are given in Table 2.

TABLE 2

Paramagnetic Parameters Obtained from EPR Spectra of the Different Cu^{2+} Samples after 2 Hours and 7 Days

| | [M] | g | $g_{//}$ | g_{\perp} | g | $g_{//}$ | g_{\perp} | $A_{//}$ (G) |
|------------------|-----------|---|----------|-------------|-------|----------|-------------|--------------|
| Cu^{2+} | 10^{-5} | - | - | - | 2.245 | - | - | - |
| | 10^{-4} | - | - | 2.07 | 2.245 | - | - | - |
| | 10^{-3} | - | 2.354 | 2.072 | - | 2.349 | 2.072 | 133 |
| | 10^{-2} | - | - | 2.07 | 2.261 | 2.345 | 2.07 | 133 |
| | 10^{-1} | - | - | 2.07 | 2.261 | 2.348 | 2.07 | 133 |

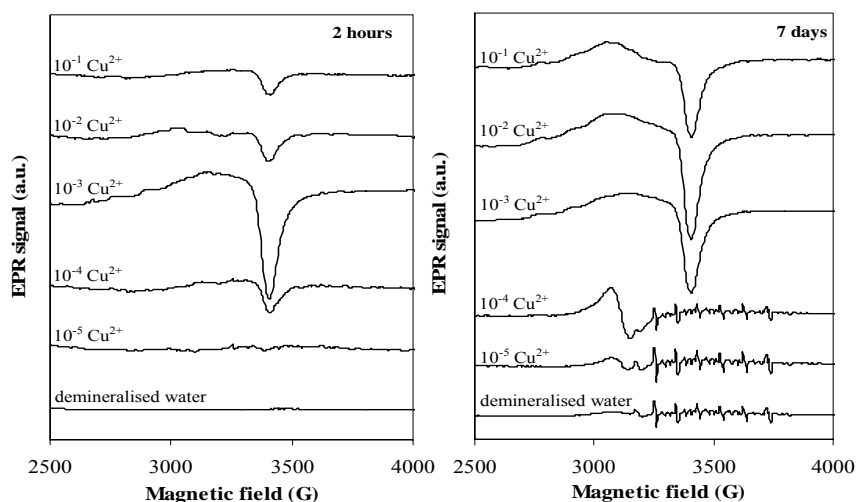


Figure 4. EPR spectra of the different Cu^{2+} /vaterite mixtures after 2 hours and 7 days of reaction.

This signal remains unchanged even after 7 days of reaction. This shows that vaterite in suspension in a 10^{-3}M cupric solution remains stable because of the surface saturation of vaterite grains by one or more layers of copper atoms responsible for the signal. The cupric ions on vaterite surface are localised in distorted octahedral sites surrounded by five ligands. For 10^{-2} and 10^{-1}M Cu^{2+} solution concentrations, EPR spectra evolve with reaction time. Thus, after 2 hours, the detected signal shows the paramagnetic characteristics of copper (II) isolated in the CaCO_3 matrix and surrounded by six coordination bonds. After 7 days of reaction, a new centred signal with $g=2.261$ is observed. This signal appears after a few hours of reaction and decreases gradually in favour of the signal $g_{//}=2.345$ and $g_{\perp}=2.07$.

Thus, this signal results from a paramagnetic resonance of Cu^{2+} ions located inside cubic calcite. Cu^{2+} ions are present in sites known as “final”, this after a complete stabilization of calcium carbonate structure.

Figure 5 shows UV-Vis/NIR spectra of pure vaterite and vaterite mixed with demineralised water after 7 days of reaction. It is clear that the two spectra are different. Thus, after 7 days, two absorption peaks are present at 2533 nm and 2337 nm, while pure vaterite presents only one broad and weak peak at 2517 nm. These various peaks correspond to carbonates vibration. In fact, in the literature (Gaffey, 1986), the calcite peaks at 2533nm and 2337 nm were attributed to the vibration of carbonates ions. The same peaks are not present for pure vaterite due to the presence of carbonates in a different environment not allowing the same vibrations. UV-Vis/NIR spectra confirm then the transformation of vaterite into cubic calcite when contacted with water.

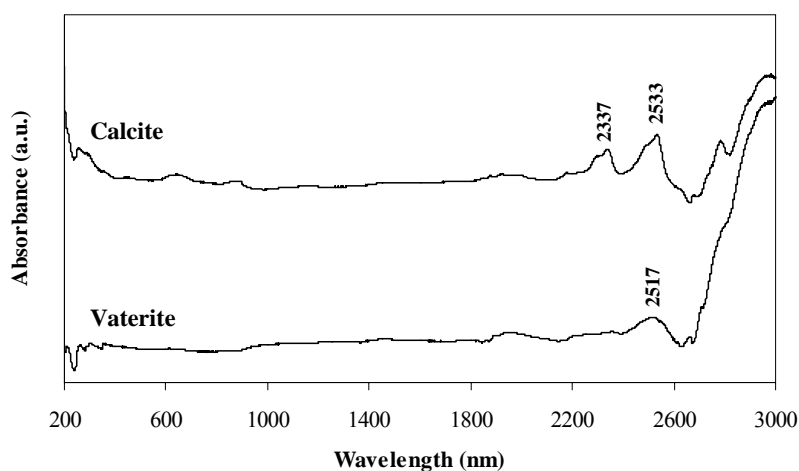


Figure 5. UV-Vis/NIR spectra of vaterite and calcite.

Figure 6 shows UV-Vis/NIR spectra of the Mn^{2+} /vaterite solids obtained after 2 hours and 7 days of reaction with different concentrations of Mn^{2+} solutions. In general, the d-d transitions of Mn^{3+} and Mn^{4+} are clearly observed in the UV-Vis field while the transitions due to Mn^{2+} ions are in theory prohibited and thus very weak (Velu *et al.*, 1999). The only observed peak is in the 250 nm region. This peak corresponds without ambiguity to the charge transfer transition from $\text{O}^{2-} \rightarrow \text{Mn}^{2+}$ (Milella *et al.*, 1998). This last is present for vaterite only after 7 days of reaction and not after 2 hours. This confirms that vaterite trap the Mn^{2+} ions during its transformation into cubic calcite, which was observed by EPR. It is also noticed that, after 7 days of reaction, cubic calcite characteristic peaks obtained for samples prepared with high Mn^{2+} concentrations solutions (10^{-2}M and 10^{-1}M) are very weak in comparison to those obtained for samples prepared with low Mn^{2+} concentration solutions (10^{-5}M , 10^{-4}M and 10^{-3}M). This observation shows that, in the presence of Mn^{2+} concentrations higher than 10^{-2}M in the aqueous media, vaterite transformation into cubic calcite is inhibited or delayed due to the formation of a manganese (II) species protection layer.

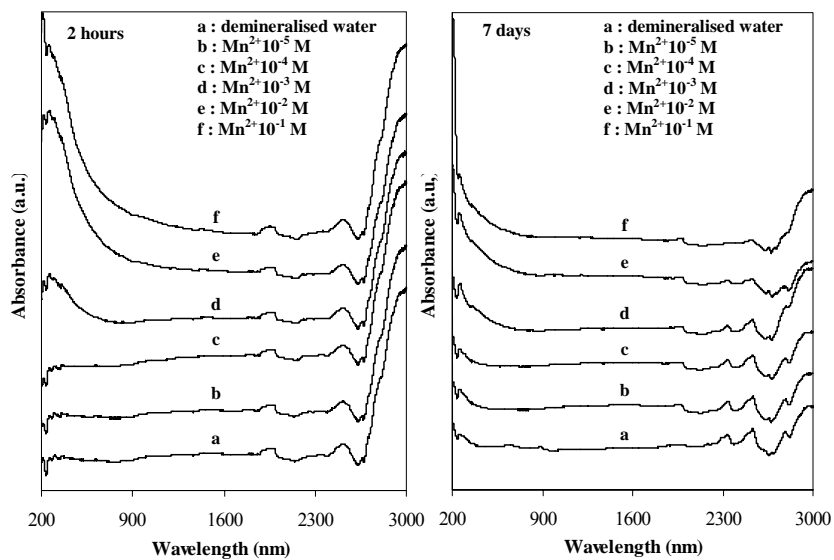


Figure 6. UV-Vis/NIR spectra of different Mn^{2+} /vaterite mixtures after 2 hours and 7 days of reaction.

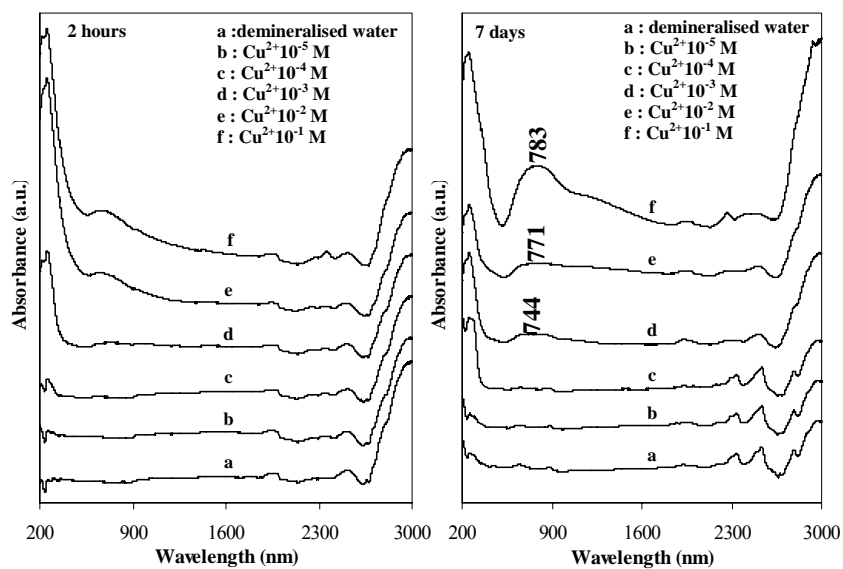


Figure 7. UV-Vis/NIR spectra of different Cu^{2+} /vaterite mixtures after 2 hours and 7 days of reaction.

Figure 7 shows UV-Vis/NIR spectra of the Cu^{2+} /vaterite solids obtained after 2 hours and 7 days of reaction with different concentrations of Cu^{2+} solutions. For Cu^{2+} /vaterite, the presence of a broad absorption peak in the UV-Vis area is observed after 2 hours and 7 days. This latter appears starting from a 10^{-3}M Cu^{2+} concentration, and its intensity is higher for the samples which reacted during 7 days, indicating the presence of a greater quantity of Cu^{2+} ions. This peak located in the 650nm to 790nm area is allotted to Cu^{2+} ions in octahedral sites presenting a strong distortion (Aboukaïs *et al.*, 1993). On the other hand, after 7 days, the absence of carbonates absorption peaks corresponding to the cubic calcite phase at 2300nm and 2500nm for 10^{-3}M and 10^{-2}M Cu^{2+} concentrations are in perfect correlation with EPR results which showed the formation of a protective coating of Cu^{2+} ions which prevents or delays the transformation of vaterite. After 7 days, and for 10^{-1}M Cu^{2+} , a shoulder is present between 1000 nm and 1400 nm and that indicates the presence of Cu (II) in square based pyramidal symmetry sites.

Figure 8 shows EPR spectra of pure vaterite and vaterite mixed with tap water during 7 days. This same signal is present after 7 days of reaction with tap water but its intensity is higher. Thus, it is obvious that during the transformation of vaterite into cubic calcite, metal ions are trapped inside the matrix which proves the capacity of vaterite to capture ions in water. All these observations confirm that the chemical behaviour of metal ions in the presence of vaterite depends on their concentration in the medium, but also on the matrix specific surface area [vaterite: $\sim 18\text{m}^2\text{g}^{-1}$] and on its evolution in time [cubic calcite: $\sim 1\text{m}^2\text{g}^{-1}$].

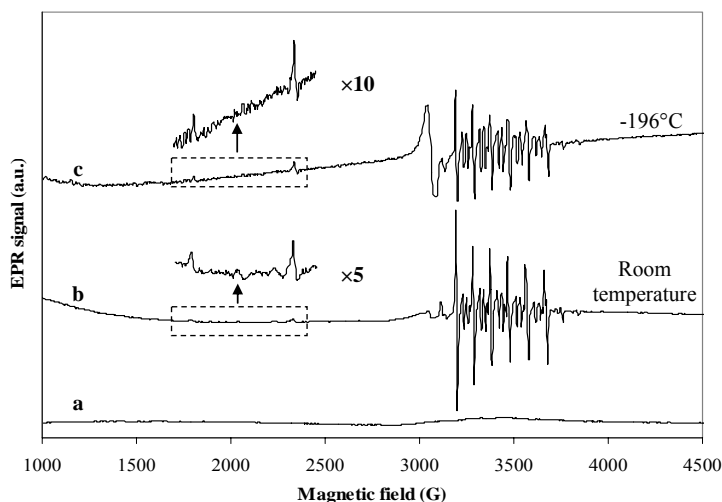


Figure 8: EPR spectra of a) pure vaterite; b) and c) vaterite/tap water 7 days.

CONCLUSION

This work permitted to highlight, by using EPR and UV-Vis/NIR spectroscopy, the capacity of vaterite to trap metal ions during its transformation into cubic calcite under the action of water. Mn^{2+} EPR signals were detected after reaction with demineralised water.

This shows the trapping efficiency of vaterite, especially in the presence of negligible metal ions quantities. Moreover, UV-Vis/NIR showed the presence of Cu (II) in strongly distorted octahedral sites.

UV-Vis/NIR technique also proved trapping of manganese (II) ions present in demineralised water. All these observations, made it possible to conclude, that the use of vaterite can be considered as not very expensive and effective solution for the depollution of metallic ions contaminated water.

REFERENCES

- Aboukaïs, A., Bennani, A., Aïssi, C.F., Wrobel, G., Guelton, M., Vedrine, J.C. 1992. Highly resolved electron paramagnetic resonance spectrum of copper(II) ion pairs in CuCe oxide. *Journal of the Chemical Society, Faraday Transactions*, 88: 615-620.
- Aboukaïs, A., Delmaire, F., Rigole, M., Hubaut, R., Mairesse, G. 1993. Compressed Cu²⁺ ions in a Bi₄V₂O₁₁ oxide matrix. 1. EPR and UV-Visible study. *Chemistry of Materials*, 5: 1819-1822.
- Baitalow, F., Wolf, G., Schmidt, H.G. 1998. Thermochemical investigations of calcium carbonate phase transitions I. Thermal activated vaterite-calcite transition. *Journal of Thermal Analysis and Calorimetry*, 52: 5-16.
- Bischoff, J.L. 1968. Catalysis, inhibition, and the calcite-aragonite problem. II-The vaterite-aragonite transformation. *American Journal of Science*, 266: 80-90.
- Boughriet, A., Ouddane, B., Fischer, J.C., Wartel, M. and Leman, G. 1992. Variability of dissolved Mn and Zn in the Seine estuary and chemical speciation of these metals in suspended matter. *Water Research*, 26: 1359-1378.
- Gaffey, S.J. 1986. Spectral reflectance of carbonate minerals in the visible and near infrared (0.35-2.55 microns): calcite, aragonite, and dolomite. *American Mineralogist*, 71: 151-162.
- Milella, F., Gallardo-Amores, J.M., Baldi, M., Busca, G. 1998. A study of Mn-Ti oxide powders and their behaviour in propane oxidation catalysis. *Journal of Materials Chemistry*, 8: 2525-2531.
- Morse, J.W., Mackenzie, F.T. 1990. *Geochemistry of sedimentary carbonates*. Elsevier Science Publishers, B.V., The Netherlands, pp.707.
- Nasrallah-Aboukaïs, N., Jacquemin, J., Decarne, C., Abi-Aad, E., Lamonier, J.F., Aboukaïs A. 2003. Transformation of vaterite into calcite in the absence and the presence of copper(II) species. *Journal of Thermal Analysis and Calorimetry*, 74: 21-27.
- Perić, J., Vučak, M., Krstulović, R., Brečević Lj., Kralj, D. 1996. Phase transformation of calcium carbonate polymorphs. *Thermochimica Acta*, 277: 175-186.
- Reeder, R.J. 1983. *Carbonates: Mineralogy and Chemistry*. Mineralogical Society of America. Reviews in Mineralogy 11. 394.
- Rivarolo, P., Frache, L., Mazzucotelli, A., Cariati, F., Pozzi, A. 1994. Spectroscopic evaluation of interactions among trace elements and biogenic carbonates in the marine environment. *Analyst*, 119: 2485-2489.
- Stumm, W. 1992. *Chemistry of the solid-water interface*. Wiley-Interscience, New York, U.S.A., pp. 428.
- Velu, S., Shah, N., Jyothi, T.M., Sivasanker, S. 1999. Effect of manganese substitution on the physicochemical properties and catalytic toluene oxidation activities of Mg–Al layered double hydroxides. *Microporous and Mesoporous Materials*, 33: 61-75.

- Wartel, M., Skiker, M., Auger, Y., Boughriet, A. 1990. Interaction of Manganese(II) with carbonates in seawater: assessment of the solubility product of $MnCO_3$ and Mn distribution coefficient between the liquid phase and $CaCO_3$ particles. *Marine Chemistry*, 29: 99-117.
- Wolf, G., Konigsberger, E., Schmidt, H.G., Knigsberger, L.C., Gamsjager, H.J. 2000. Thermodynamic aspects of the vaterite-calcite phase transition. *Journal of Thermal Analysis and Calorimetry*, 60: 463-472.